

## Research Paper

## Characterization of Combustion in Cylindrical Meso-Scale Combustor with Wire Mesh Flame Holder as Initiation of Energy Source for Future Vehicles

Andi Sanata<sup>1</sup>✉, Nasrul Ilminnafik<sup>1</sup>, Muhammad Maulana Asyhar<sup>1</sup>, Hendry Y. Nanlohy<sup>2</sup>, Franciscus Xaverius Kristianta<sup>1</sup>, Imam Sholahuddin<sup>1</sup>

<sup>1</sup> Energy Conversion Laboratory, Department of Mechanical Engineering, Jember University, Jember 68121, Indonesia

<sup>2</sup> Department of Mechanical Engineering, Jayapura University of Science and Technology, Jayapura 99351, Indonesia

✉ andisanata@unej.ac.id

🌐 <https://doi.org/10.31603/ae.10715>

Published by Automotive Laboratory of Universitas Muhammadiyah Magelang

### Abstract

#### Article Info

Submitted:

19/12/2023

Revised:

08/04/2024

Accepted:

27/04/2024

Online first:

27/04/2024

The research aims to analyze and reveal combustion characteristics in a Cylindrical Meso Scale (CMS) Combustor with a wire mesh flame holder as a reference for designing a compact, efficient, and high-density energy source for future vehicles. This experiment analyzes the combustion phenomena's of a butane gas (C<sub>4</sub>H<sub>10</sub>)-air mixture in a cylindrical meso-scale (CMS) combustor with the addition of wire mesh flame holder on the stability of the combustion flame, as initiation of future vehicle energy source. The diameter of the CMS combustor with wire mesh flame holder is varied to give an idea of the effect of heat loss on the combustion flame's characteristics. The results show that the wire mesh as a flame holder is essential in the combustion stabilization mechanism. A stable flame can be stabilized in a CMS combustor with wire mesh. Variations in the diameter of the CMS combustor will result in variations in the surface-to-volume ratio, heat loss, and contact area of the wire mesh flame holder. At a large diameter, it produces the characteristics of a combustion flame with a more stable flame stability limit than a smaller diameter, a dimmer flame visualization than a smaller diameter at the same air and fuel discharge, a more distributed flame mode map area than the smaller diameter, lower flame temperature and combustor wall temperature than the smaller diameter, and relatively higher energy output than the smaller diameter.

**Keywords:** CMS combustor; Flame holder; Flame stability; Future vehicle energy source; Wire mesh

### 1. Introduction

A compact, efficient, and high-density energy source is crucial for converting conventional and electric/smart vehicles and driving future energy sources [1]–[3]. Batteries have long been expected to fulfill this role. However, their development faces significant obstacles, including low energy density, prolonged recharging times, and environmental concerns about battery waste [4]–[6]. In line with this, the miniaturization of energy generation from combustion results on a small scale (micro/meso-scale combustion) known as a

Micro Power Generator (MPG) in the application of Micro-Thermophotovoltaic technology has the potential to be developed as a compact, efficient, and high-density energy source. MPG takes energy from a highly efficient combustion process at the micro/meso scale as a source of energy production to drive MPG, which has many advantages over batteries [7], [8]. The results obtained by the energy density produced by burning hydrocarbon fuel to drive MPG are more significant than the results of the battery chemical process [9].



This work is licensed under a Creative Commons Attribution-NonCommercial 4.0 International License.

The MPG system design is composed of a micro/meso-scale combustor as a converter of fuel chemical energy into heat energy and a module for converting heat energy into electrical energy, namely Micro-Thermophotovoltaic Power Systems [10]. Micro/meso-scale combustor, as the main component of MPG, plays an essential role in supporting the system to produce a stable flame during combustion. The combustion required for MPG to release the energy bound in the fuel requires unique criteria, namely that combustion is carried out in micro/meso scale volume control. Because the size is tiny, using micro/meso scale combustors faces many difficulties in obtaining flame stability [11].

Previous research indicates that reducing the combustor's size increases the heat loss ratio due to the high surface-to-volume ratio of the micro/meso-scale combustor. This condition causes an unstable flame due to thermal quenching around the combustor walls and increased heat loss on the combustor walls, thus triggering fire extinguishing [12]. The short residence times and inadequate reaction times can make the condition worse [13]. Researchers have devised different treatments for small-scale combustors to improve flame stability. These include using external heating [14]–[16], heat-recirculating [17]–[19] porous media [20], [21], catalytic materials [22]–[24], bluff body [25], Biogas as fuel [26], flame holder [27], and using backward-facing step flame holder [8], [28]. The use of a backward-facing step as a flame holder in a micro/meso-scale combustor can increase the stability of the combustion flame. Increasing the diameter of the combustion chamber of a micro- or meso-scale combustor with a backward-facing step flame holder will increase reactant mixing and reduce heat loss, thereby increasing the stability of the combustion flame. Increasing the size of the backward-facing step on a micro/meso-scale combustor with a backward-facing step flame holder at a constant diameter of the micro/meso-scale combustor combustion chamber will reduce the stability of the combustion flame. Increasing the size of the backward-facing step causes an increase in the recirculation flow, reactant inlet velocity, velocity gradient, and shear stress, which have an essential influence on flame stability. The large reactant inlet velocity, shear stress, and recirculation flow tend to make the flame exit, causing heat transfer

from the flame to the combustion chamber walls, which extinguishes the flame. The flame stabilization mechanism through flow recirculation is reduced due to the high reactant inlet velocity and shear stress effects. The flame can be stabilized backward-facing step at a small backward-facing step. The small backward-facing step stabilizes the flame through a heat recovery mechanism and flow recirculation that acts as a flame holder in the cylindrical mesoscale combustion chamber [29].

The idea used to stabilize the flame in this research is to create a CMS combustor passage with a wire mesh flame holder. Wire mesh is one type of flame holder that will be researched and used in CMS combustion chambers to increase the stability of the combustion flame. Wire mesh as a flame holder is like a filter in the middle of the CMS combustor path. Wire mesh can recirculate heat (heat recirculation) from the flame to the reactants (preheating) through conduction on the combustion chamber walls. The heat generated from the combustion process is partly convected to the walls of the combustion chamber. Some of the heat is convected into the environment as heat loss, and the remainder is channeled to the upstream walls of the combustion chamber. Some of the heat that flows to the walls of the combustion chamber is then convected into the reactant flow for the initial heating process of the reactants, and the other part is flowed to the wire mesh. The hot part that flows through the wire mesh is also convected to the reactants for further preheating, or if the temperature of the wire mesh is high enough, it can also function as an igniter. The wire mesh on the combustor is expected to be able to function as a flame holder and increase recirculation of fuel-air flow and heat flow from the flame to the reactants so that better flame stability is obtained. This research aims to obtain the combustion characteristics of a CMS combustor with a wire mesh flame holder to obtain a compact, efficient, and high-density energy source device as the initiation of a future vehicle energy source.

## 2. Methods

**Figure 1** depicts the testing equipment utilized in this study. The fuel employed is butane gas ( $C_4H_{10}$ ), and air is the oxidizing agent. The fuel supply is pressurized, and its flow rate is

determined through a flowmeter designed for butane gas (Kofloc, RK 1250, maximum flow rate: 20 mL/min). On the other hand, the air supply is sourced from an air compressor, and its flow rate is measured via a flowmeter for air (Kofloc, RK 1250, maximum flow rate: 500 mL/min).

The geometric details of a CMS combustor with a wire mesh flame holder are shown in

Figure 2 and Figure 3. The combustor is made of copper at the inlet and pyrex glass tube at the outlet, with wire mesh 60 stainless steel SUS 304. The diameter of the combustor is varied to obtain the value of the surface-to-volume ratio, which can affect the flame stability on a CMS combustor. Surface-to-volume ratio values can be seen in Table 1.

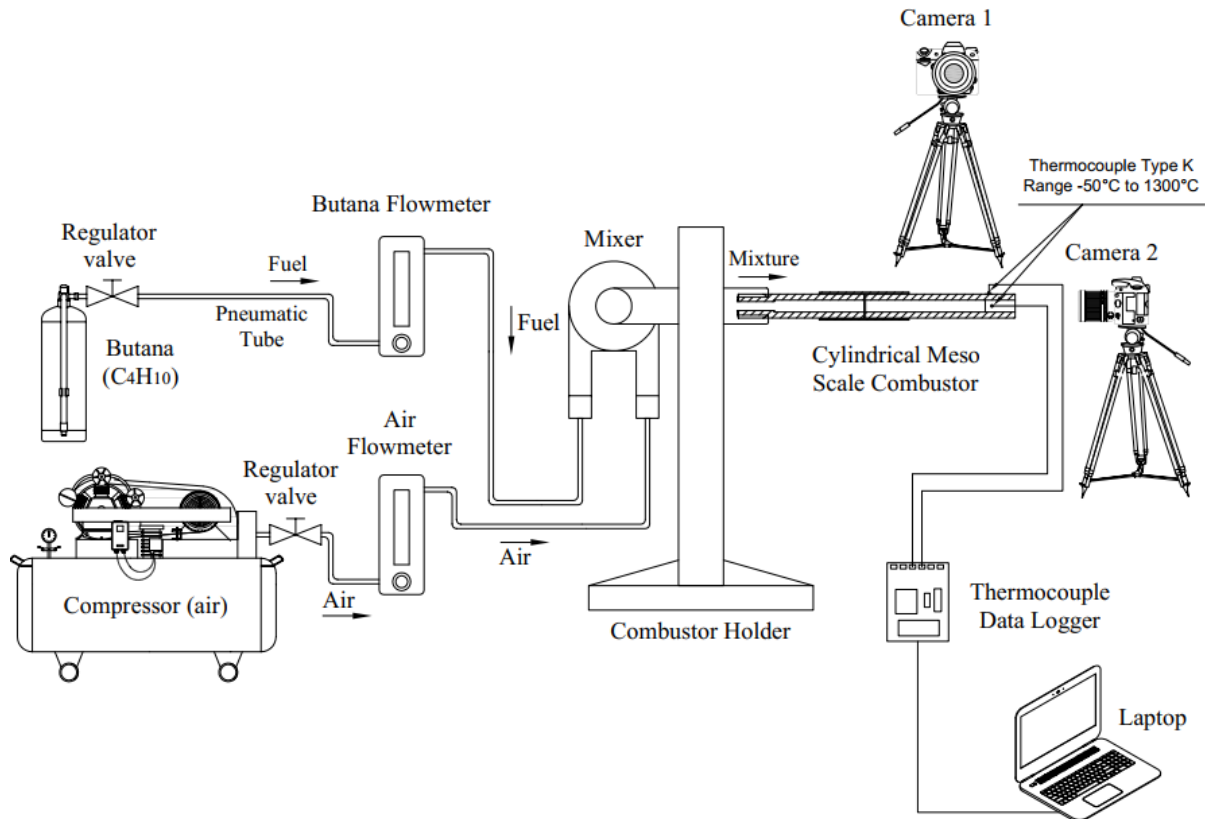


Figure 1. Schematic test equipment

Table 1. Variations in the size of the combustor geometry

Diameter (D) mm	Length (L) mm	Surface (S) mm <sup>2</sup>	Volume (V) mm <sup>3</sup>	S/V
4	10	125.60	125.60	1.00
5	10	157.00	196.25	0.80
6	10	188.40	282.60	0.67

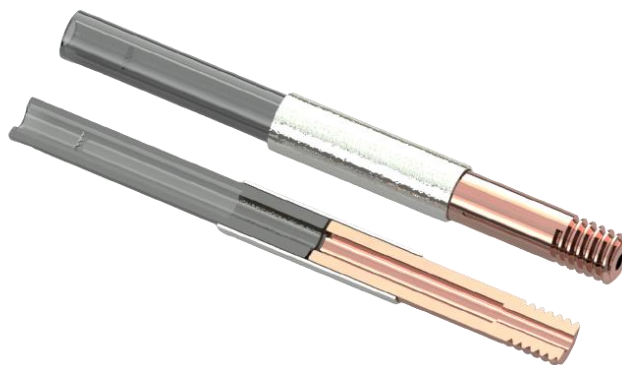
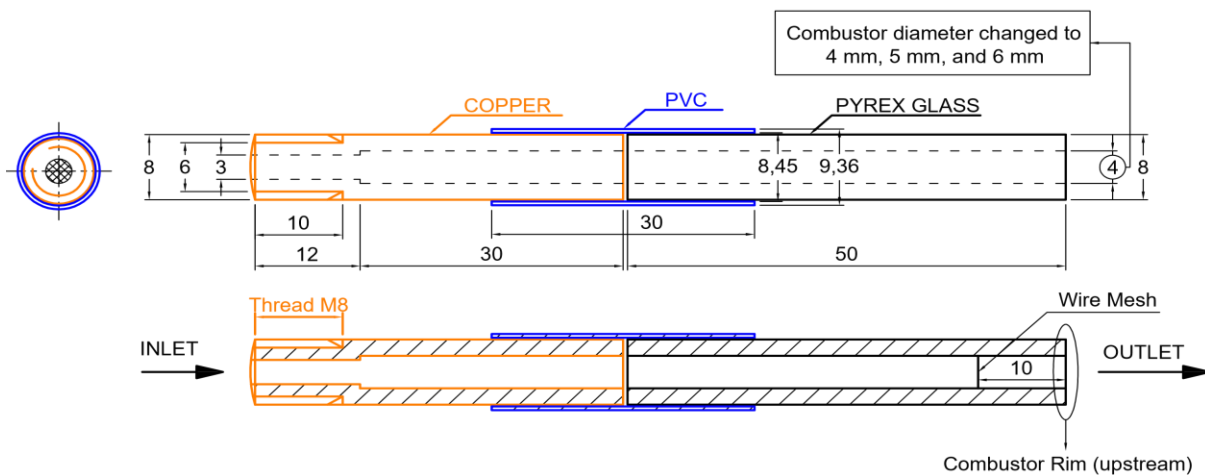


Figure 2. Schematic of a CMS combustor with wire mesh



**Figure 3.** Schematic three dimensions of a CMS combustor (units in mm)

The fuel supply to the combustor is facilitated through a pressurized tube, while an air compressor provides air. A Kofloc RK 1250 flowmeter regulates the butane gas and air flow rates, measuring between 2-20 and 50-500 mL/min, respectively. The fuel and airflow rates can be adjusted within the minimum and maximum values to maintain a stable flame in the combustor. Before entering the combustion chamber, the air and fuel are mixed to create a premixed mixture. The lighter on the combustor's rim is then utilized to ignite the premixed mixture, which propagates and stabilizes within the combustion chamber at the allowable air and fuel flow rate. If the air and fuel flow rate falls outside the specified range, the flame may go out, flashback, or blow off.

The flame was photographed using a digital camera, capturing the combustor's front and side views. The Flame was analyzed and classified into several modes, including Flame at the combustor rim, Flame in the combustor, Flame near the mesh, Flashback, and No ignition. Flame mode was presented in a graph showing the reactants' flow rate, helping to obtain flame mode maps.

Type K thermocouple with a temperature range of  $-50\text{ }^{\circ}\text{C}$  to  $1300\text{ }^{\circ}\text{C}$  and a data logger are used to obtain flame and combustor wall temperature readings. The thermocouple is placed in the combustion chamber to measure flame temperature and on the combustor wall to measure the combustor wall temperature, as shown in [Figure 4](#). The reading results are processed to calculate energy, which is then used to analyze heat loss caused by variations in the diameter of the combustion chamber.

### 3. Result dan Discussion

[Figure 5](#) shows a graph of the flame stability limit of the combustion of premixed butane and air in a CMS combustor with variations in the diameter of the combustor. The flame stability limit indicates that the flame can burn stably at a position close to the wire mesh (or at a distance of  $\leq 1\text{ mm}$  from the wire mesh).

[Figure 5](#) shows that the lowest equivalence ratio ( $\phi$ ) for a combustor diameter of 4 mm is 0.67 with a reactant velocity ( $v$ ) of 29.08 cm/s, and the highest equivalence ratio is 1.43 with a reactant velocity of 17.28 cm/s. While the lowest equivalence ratio at a 5 mm combustor diameter was 0.58 with a reactant velocity of 21.16 cm/s, the highest equivalence ratio was 1.44 with a reactant velocity of 18.53 cm/s. Furthermore, the lowest equivalence ratio at a 6 mm combustor diameter is 0.56 with a reactant velocity of 19.01 cm/s, and the highest equivalence ratio is 1.62 with a reactant velocity of 11.45 cm/s.

[Figure 5](#) shows that the combustor diameter of 6 mm produces the most extensive range of interval equivalence ratios compared to the diameters of 4 mm and 5 mm. The smaller the diameter of the combustor with a constant length, the greater the surface-to-volume ratio, so the heat loss that occurs increases [30]. Increased heat loss can reduce the stability of the flame. Wire mesh as a flame holder can increase the stability of the flame. The larger the cross-section of the combustor, the greater the contact area of the wire mesh used. The larger the contact area of the wire mesh will increase the preheating of the reactants. So that the greater the contact area of the wire mesh will increase the stability of the flame. This

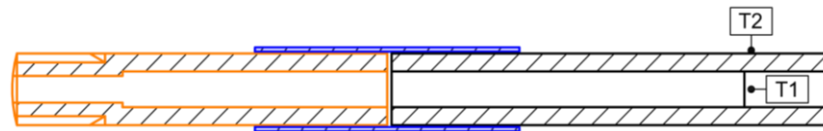


Figure 4. Schematic of temperature-taking

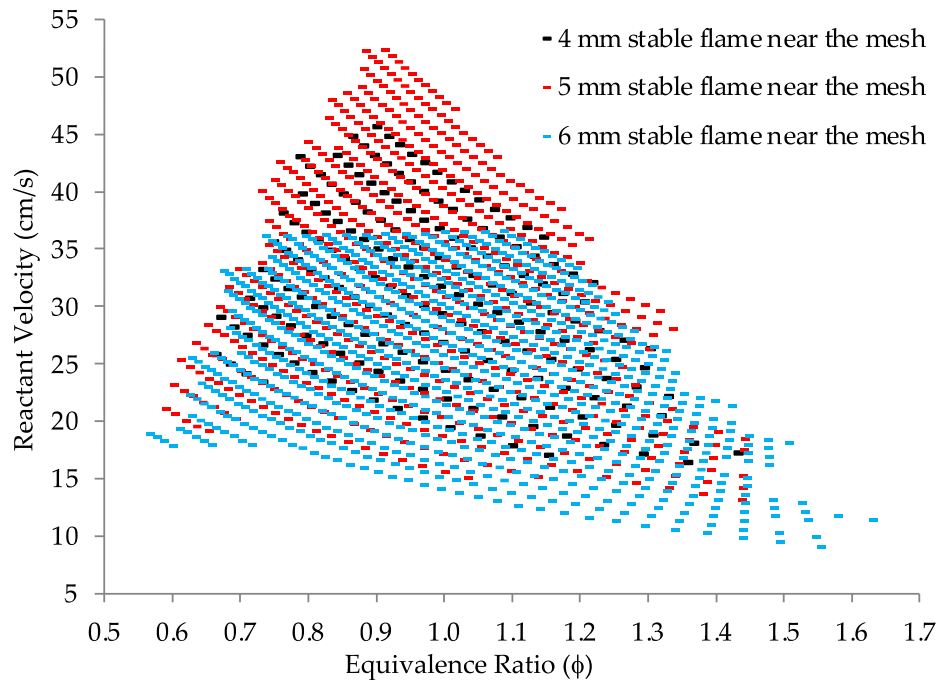


Figure 5. Flame stability limit for variations in diameter of CMS combustor

analysis is grounded on earlier investigations on burning crude vegetable oil set alight using a coil heater powered by electricity [31]. The current research aims to provide a fresh viewpoint on the subject matter [32], [33]. The combustor diameter of 6 mm produces combustion with a minor heat loss because the combustor diameter of 6 mm has a minor surface-to-volume ratio compared to the diameters of 4 mm and 5 mm. The combustor diameter of 6 mm has the most prominent wire mesh contact area. This results in preheating the reactants occurring higher than the combustor diameters of 4 mm and 5 mm. Therefore, the combustor diameter of 6 mm produces the most expansive flame stability limit area with the lowest heat loss compared to the 4 mm and 5 mm combustor diameters.

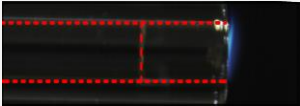

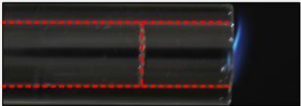


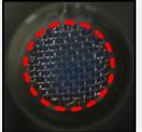
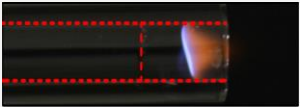
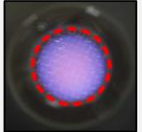
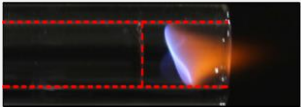
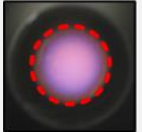
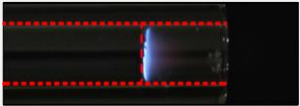
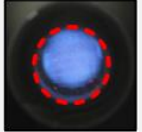
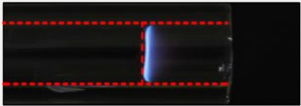
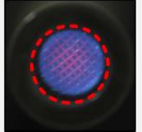
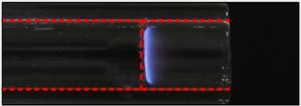
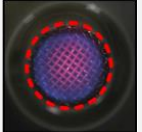
CMS combustor of varied diameters was used to burn the butane-air mixture, and the resulting flame is visualized in Table 2. The flame exhibited stable modes in different locations, such as at the edge, near the mesh, and inside the combustor. Table 2 shows several flame mode conditions that are formed at the same equivalence ratio for each

flame mode as a comparison of the visualization of the flame that occurs with variations in the diameter of the combustor. Table 2 shows that the different diameters of the combustor produce different flame modes with the same equivalence ratio for each of the conditions in which the flame mode is formed. Variations in the diameter of the combustor cause the difference in flame mode [34], [35]. Variations in combustor diameter can result in differences in reactant flow rates, heat loss, and differences in the intensity of preheating of the fuel by the wire mesh in each diameter variation. The larger diameter of the combustor will decrease the speed of the reactants and increase the fuel residence time [36], [37]. When the speed of the reactants decreases, the reactants to supply the combustion reaction decrease and cause the flame to become thinner. Flame mode stable flame at the combustor rim for a combustor diameter of 4 mm produces a thicker and brighter flame shape. Then the more significant the diameter of the combustor, which is 5 mm and 6 mm, the shape of the flame is getting thinner and dimmer. This phenomenon occurs due to the

reactants' decreasing velocity and inadequate fuel preheating; the present analysis builds upon prior research from diverse perspectives, incorporating technical intricacies [38]. If the contact area of the wire mesh increases, but the speed of the reactants decreases, then the preheating temperature of the reactants will decrease due to the spreading heat, resulting in inadequate preheating of the reactants [39].

Furthermore, flame mode stable flame near the mesh is formed with the position of the flame attached to the mesh with a distance of  $\leq 1$  mm. As seen in **Table 2**, the flame tends to be thicker for a flame near the mesh diameter of 4 mm. At 5 mm and 6 mm in diameter, the shape of the flame gets thinner and dimmer. This phenomenon occurs due to the reactants' decreasing velocity and inadequate fuel preheating.

**Table 2.** Flame visualization for various diameters of CMS combustors

No	Flame Mode	Diameter 4 mm	Diameter 5 mm	Diameter 6 mm
1.	Stable flame at the combustor rim	$\phi = 1.41$ $v = 10.61$ cm/s  Side view RGB (%): 17.12; 31.46; 51.42  Front view RGB (%): 23.47; 33.41; 43.11	$\phi = 1.41$ $v = 6.79$ cm/s  Side view RGB (%): 20.85; 30.38; 48.77  Front view RGB (%): 27.88; 32.59; 39.52	$\phi = 1.41$ $v = 4.71$ cm/s  Side view RGB (%): 21.75; 29.60; 48.64  Front view RGB (%): 28.71; 32.32; 38.96
2.	Stable flame in the combustor	$\phi = 0.73$ $v = 36.48$ cm/s  Side view RGB (%): 42.47; 28.43; 29.09  Front view RGB (%): 31.39; 25.92; 42.75	$\phi = 0.73$ $v = 35.87$ cm/s  Side view RGB (%): 45.52; 28.35; 26.12  Front view RGB (%): 38.15; 25.85; 35.92	
3.	Stable flame near the mesh	$\phi = 1$ $v = 40.91$ cm/s  Side view RGB (%): 23.56; 31.16; 46.81  Front view RGB (%): 22.07; 29.65; 48.27	$\phi = 1$ $v = 26.18$ cm/s  Side view RGB (%): 24.39; 31.06; 45.36  Front view RGB (%): 26.65; 25.18; 48.16	$\phi = 1$ $v = 18.18$ cm/s  Side view RGB (%): 25.07; 28.12; 44.44  Front view RGB (%): 34.47; 22.04; 43.48

The stable flame mode in the combustor occurs when the flame is situated within the reaction zone at a distance greater than 1 mm from either end of the combustor. When the combustor diameter is 4 mm, the flame position tends to be further from the mesh. As the diameter increases to 5 mm, the flame moves closer to the mesh. However, at a diameter of 6 mm, the reactants' velocity decreases, and there is insufficient fuel preheating, resulting in no flame in the combustor.

Figure 6 to Figure 8 depict flame mode maps for the combustion of a premixed butane-air mixture in a CMS combustor. These maps show variations in combustor diameter and detail the reactant flow velocity to equivalence ratio ( $v-\phi$ ) of the different flame modes of combustion. The maps cover different fuel-air mixture equivalence ratio ranges and possible reactant flow rates. Figure 6 to Figure 8 illustrates the areas where stable flame modes occur at the combustor rim, steady flame in the combustor, stable flame near the mesh, and flashback.

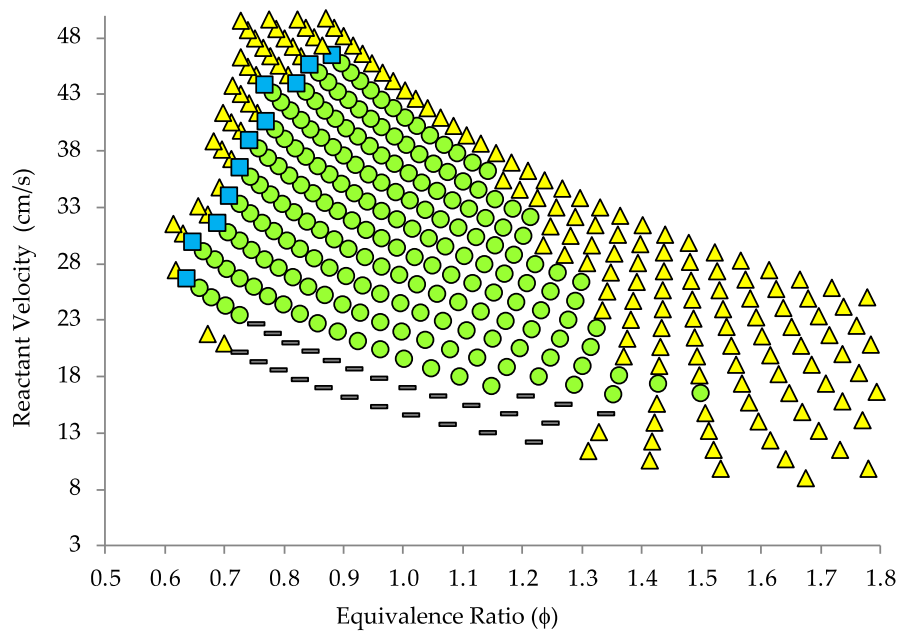


Figure 6. Flame mode map for 4 mm diameter combustor

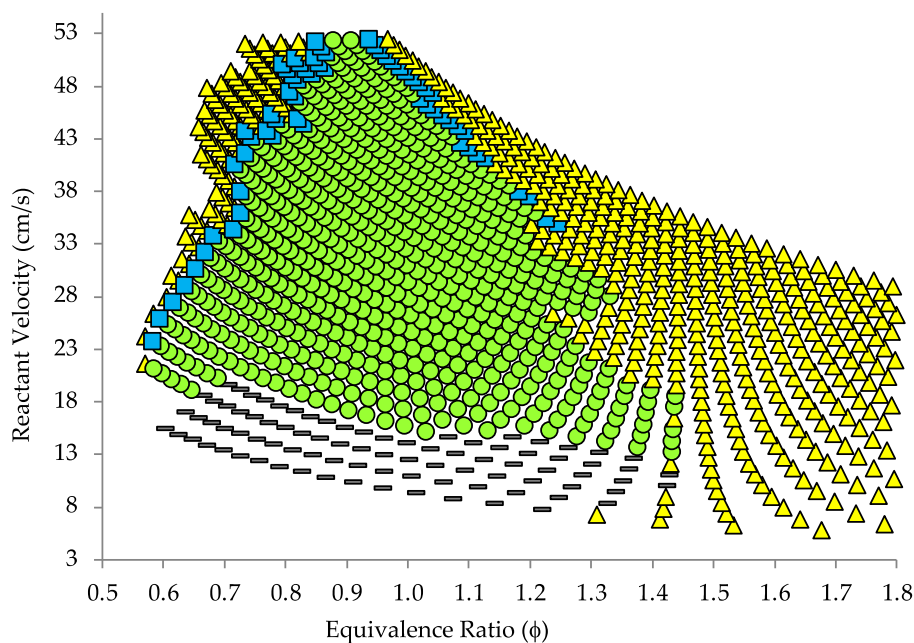
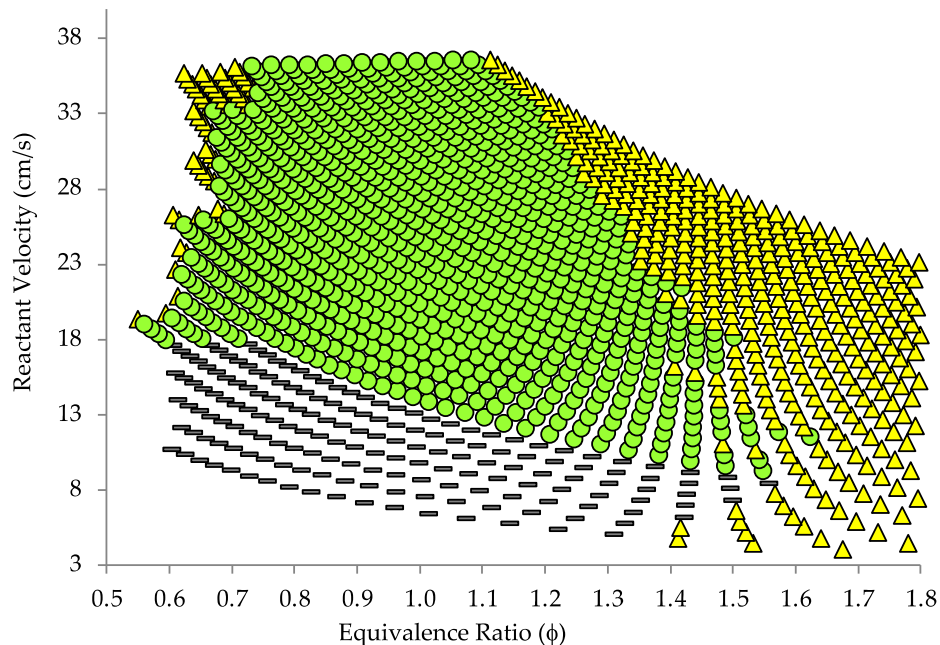


Figure 7. Flame mode map for 5 mm diameter combustor



**Figure 8.** Flame mode map for 6 mm diameter combustor

Flame mode maps formed on the  $v$ - $\phi$  graph vary according to the flow velocity of reactants and equivalence ratio for each variation in the diameter of the CMS combustor, as shown in [Figure 6](#) to [Figure 8](#). These maps indicate five characteristic flame mode areas: stable flame at the combustor rim, steady flame near the mesh, stable flame in the combustor, flashback, and no ignition at the reactant flow velocity to the equivalence ratio ( $v$ - $\phi$ ). The combustor's diameter and the wire mesh's contact area affect the occurrence of these flame modes. Variations in flow velocity of the reactants, heat loss due to combustor diameter changes, and reactant preheating due to wire mesh contact area changes form different flame mode maps at the same equivalence ratio for each combustor diameter. Flame mode distribution on the map increases with larger combustor diameters. Flame modes with no ignition and flashback are not desirable during heat generation from a CMS combustor. [Figure 6](#) to [Figure 8](#) explain the process during operation, and combustor diameter selection can be made based on these flame mode maps. The 4 mm and 5 mm diameters are the most exciting conditions because they exhibit various flame behaviors (more variation than the 6 mm diameter).

The data in [Figure 6](#) to [Figure 8](#) shows that a stable flame can be formed at the rim of the

combustor. This happens in all variations of the combustor's diameter under different conditions like low and high reactant velocities and equivalence ratios. However, the ambient air condition affects the equivalence ratio, making the flame poorer and less effective when expelled through the combustor channel. When the combustor diameter is smaller, the flame becomes more elongated and pushed towards the combustor rim [40]. For high reactant velocities, the flame drifts along the combustor rim. A stable flame at the combustor rim is also formed under different conditions, such as low and high equivalence ratios for low and high reactant velocities. Notably, flames with low and high equivalence ratios can burn stably at high reactant velocities and continue to burn on the combustor rim. This happens due to the effect of environmental air diffusion [41].

Additionally, alterations in the flow rate of the reactants and equivalence ratio can result in a transition of the flame to a stable flame mode close to the mesh. The stable flame mode is situated firmly and adheres to the wire mesh area. Combustors with diameters of 4 mm, 5 mm, and 6 mm are capable of producing a stable flame near the mesh due to the formation of a flat area between the velocity of the reactants and the stability of the flame. For the stable flame area close to the mesh, the lowest equivalence ratio at



a 4 mm combustor diameter was 0.67 with a reactant speed of 29.08 cm/s, while the highest equivalence ratio was 1.43 with a reactant speed of 17.28 cm/s. Similarly, at a 5 mm combustor diameter, the lowest equivalence ratio was 0.58 with a reactant speed of 21.16 cm/s, while the highest equivalence ratio was 1.44 with a reactant speed of 18.53 cm/s.

Furthermore, at a 6 mm combustor diameter, the lowest equivalence ratio was 0.56 with a reactant speed of 19.01 cm/s, while the highest equivalence ratio was 1.62 with a reactant speed of 11.45 cm/s. These outcomes indicate that a stable flame near the mesh can occur at an equivalence ratio of 1 and in the surrounding area that is not too fuel-rich or too fuel-poor. However, flashback will occur at an equivalence ratio of around one and at a reactant velocity that is too low [42]. If the reactant velocity is too high, it can cause the flame to enter the stable flame in the combustor or the steady flame at the combustor rim mode. Combustor diameters of 4 mm, 5 mm, and 6 mm, respectively, resulting in a high flame area of the stable flame near the mesh. The larger the diameter of the combustor causes a stable flame near the mesh to form in areas where the reactant velocity tends to be low [43]. The results of this study indicate that the flame area of a stable flame near the mesh of combustor diameters of 4 mm, 5 mm, and 6 mm can be formed at the lowest speed, respectively, namely: 16.41 cm/s, 13.20 cm/s, and 9.20 cm/s. However, the results of this study also show that the fluctuation of the highest reactant velocity ratio is in the area of the stable flame near the mesh. The highest reactant velocity in the stable flame near the mesh combustor diameter of 4 mm was 45.69 cm/s, the 5 mm combustor diameter was 52.35 cm/s, and the 6 mm combustor diameter was 36.56 cm/s. These fluctuations are caused by a decrease in heat loss and an increase in the preheating intensity of the fuel at a combustor diameter of 5 mm. Even though it is affected by the decreasing speed of the reactants, the speed is not proportional to the decreased heat loss and the increased preheating intensity of the fuel.

Furthermore, a steady flame is formed in the combustor channel during combustor mode, which is stable in the fuel-poor equivalence ratio region and the medium to high reactant velocity region for diameters of 4mm and 5mm. The

flame's stability depends on the combustor's diameter, as larger diameters lead to slower reactant velocities and more stable flames. However, if the speed of the reactants is too low, the steady flame in combustor mode may not be formed; instead, the flame remains stable near the mesh mode [44].

Meanwhile, **Figure 9** and **Figure 10** depicts a graph that illustrates the variations in temperature between the flame and the combustor walls during the combustion of a premixed butane and air mixture in a CMS combustor for different combustor diameters. The graph shows the flame's temperature and the combustor wall's temperature for three variations of the combustor diameter at an equivalence ratio of 1 and with possible reactant flow rates. The graph provides details of the temperature variation concerning the diameter of the combustor in the flame mode stable flame near the mesh condition.

**Figure 11** shows a graph of the energy output of butane and air combustion in a CMS combustor with variations in the size of the combustor diameter. The energy output is detailed in the energy-to-diameter graph for the flame mode stable flame near the mesh conditions for three different combustor diameters at an equivalence ratio of 1 and the possible reactant flow rates.

As seen in the graph in **Figure 9**, a combustor diameter of 4 mm produces a flame temperature of 1066.30 °C, a combustor diameter of 5 mm produces a flame temperature of 1094.90 °C, and a combustor diameter of 6 mm produces a flame temperature of 972.05 °C. Meanwhile, in the graph in **Figure 10**, a combustor diameter of 4 mm produces a wall temperature of 324.33 °C, a combustor diameter of 5 mm produces a wall temperature of 335.34 °C, and a combustor diameter of 6 mm produces a wall temperature of 301.14 °C. Then in **Figure 11**, a combustor diameter of 4 mm produces an energy output of 12175.12 J/s, a combustor diameter of 5 mm produces an energy output of 14697.88 J/s, and a combustor diameter of 6 mm produces an energy output of 14938.39 J/s. The flame's temperature and the combustor wall temperature were taken for variations in combustor diameter of 4 mm, 5 mm, and 6 mm at the same flow rate, namely: air discharge 9.69 ml/min and fuel 298.63 ml/min.

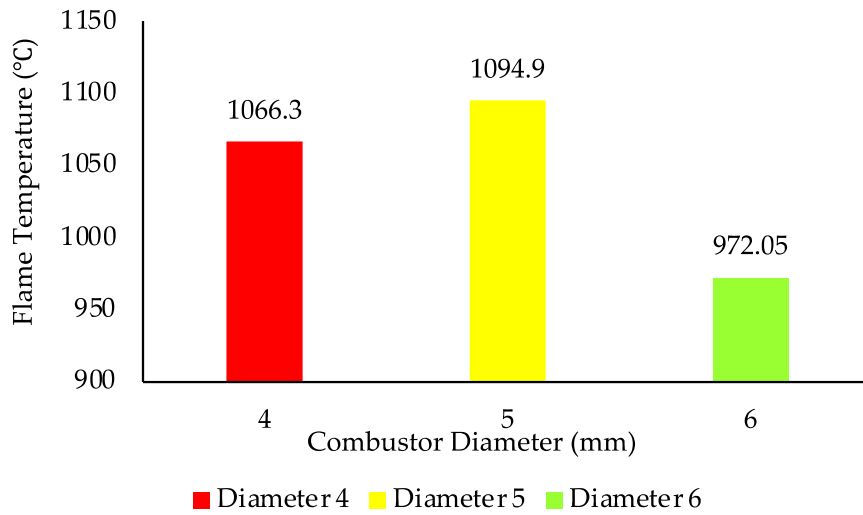


Figure 9. Flame temperature for variations in diameter of CMS combustor

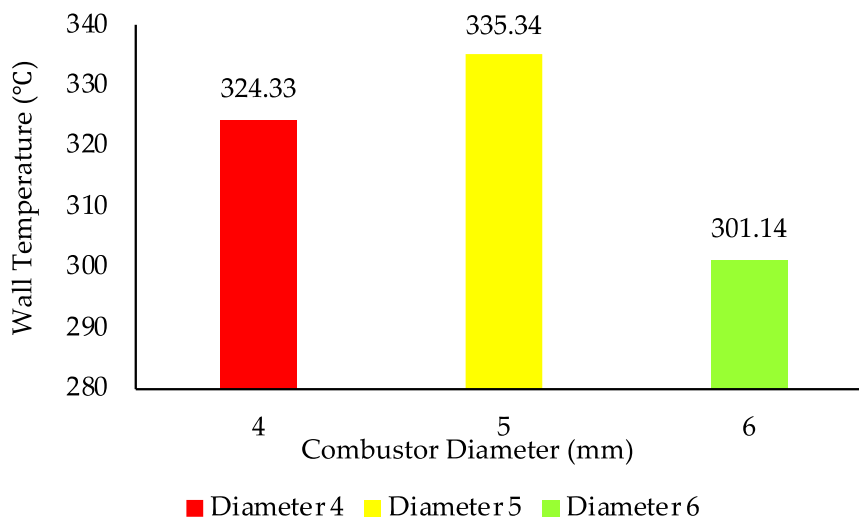


Figure 10. Combustor wall temperature for various CMS combustor diameters

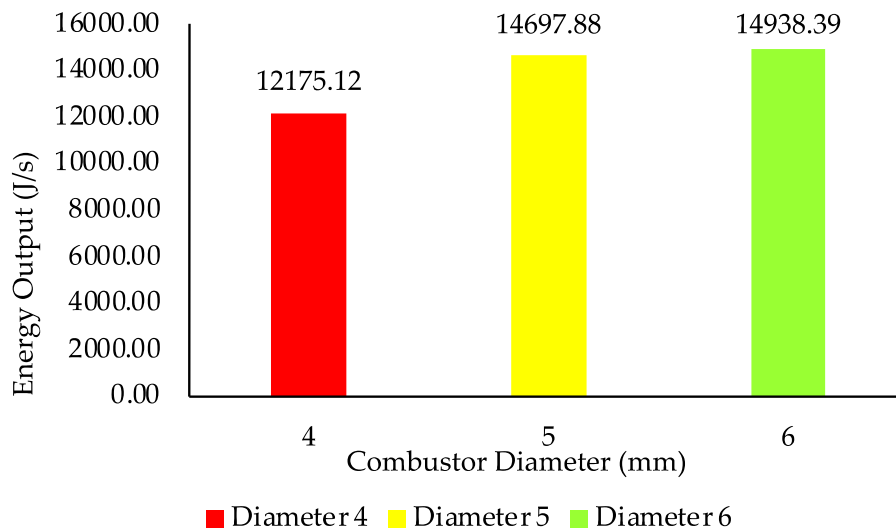


Figure 11. Energy output for varying the diameter of a CMS combustor

Figure 9 to Figure 11 shows that different combustor diameters produce different flame temperatures, combustor wall temperatures, and energy output with the same equivalence ratio for each variation of combustor diameter. Differences in temperature and energy output are caused by combustor and wire mesh diameters, resulting in differences in reactant flow rates, heat loss, and fuel preheating intensity in each variation of combustor diameter.

As seen in Figure 9 and Figure 10, there is an increase in flame temperature and combustor wall temperature from 4 mm to 5 mm diameter of the combustor. The temperature increase is due to decreased heat loss and increased fuel preheating intensity. Even though it is influenced by the decreasing velocity of the reactants so that it can reduce the temperature of the flame and the temperature of the combustor wall, the speed of the reactants is not proportional to the decreased heat loss and the increased preheating intensity of the fuel [36], [45]. While the temperature of the flame and the temperature of the combustor wall from 5 mm to 6 mm diameter of the combustor decreased. The decrease in temperature is caused by the speed of the reactants, which is lower than the diameter of 4 mm to 5 mm. Even though the heat loss decreased and the preheating intensity of the fuel increased from a combustor diameter of 5 mm to 6 mm, this was not proportional to the decreased reactant velocity.

Seen in Figure 11 shows a graph of energy output. Similar to the increase in flame temperature and combustor wall temperature from 4 mm to 5 mm diameter of the combustor, the energy output in the combustor diameter has also increased due to decreased heat loss and increased preheating intensity of the fuel. However, in contrast to the temperature of the flame and combustor wall temperature, which decreased from 5 mm to 6 mm in diameter, the energy output in the combustor diameter experienced a less significant increase than the increase in energy output in the 4 mm to 5 mm combustor diameter. This happens because calculations prove that the smaller the diameter of the combustor with a constant length, the greater the surface-to-volume ratio so that the heat loss that occurs increases and vice versa. This also indicates that there is a possibility of a decrease in energy output at combustor diameters > 6 mm due

to the effect of reactant velocity, which dominates rather than the effect of heat loss and the intensity of preheating of the fuel.

#### 4. Conclusion

Wire mesh, as a flame holder, is essential in the combustion stabilization mechanism. A stable flame can be stabilized in a CMS combustor with a wire mesh flame holder. Increasing the diameter of the CMS combustor reduces heat loss and produces more stable flames with higher energy output. However, the flame visualization is dimmer than with smaller diameters.

#### Acknowledgements

Thanks are expressed to The Institute for Research and Community Service (LP2M) Jember University, which has supported this work.

---

#### Author's Declaration

##### Authors' contributions and responsibilities

The authors made substantial contributions to the conception and design of the study. The authors took responsibility for data analysis, interpretation and discussion of results. The authors read and approved the final manuscript.

##### Funding

No funding information from the authors

##### Availability of data and materials

All data are available from the authors.

##### Competing interests

The authors declare no competing interest.

##### Additional information

No additional information from the authors.

---

#### References

- [1] A. Jannesar Niri, G. A. Poelzer, S. E. Zhang, J. Rosenkranz, M. Pettersson, and Y. Ghorbani, "Sustainability challenges throughout the electric vehicle battery value chain," *Renewable and Sustainable Energy Reviews*, vol. 191, p. 114176, Mar. 2024, doi: 10.1016/j.rser.2023.114176.
- [2] S. Marianingsih and F. Utamingrum, "Comparison of Support Vector Machine Classifier and Naïve Bayes Classifier on Road Surface Type Classification," *3rd International Conference on Sustainable Information Engineering and Technology, SIET 2018 -*

- Proceedings*, pp. 48–53, 2018, doi: 10.1109/siet.2018.8693113.
- [3] Suyatno, H. Riupassa, S. Marianingsih, and H. Y. Nanlohy, “Characteristics of SI engine fueled with BE50-Isocetane blends with different ignition timings,” *Heliyon*, vol. 9, no. 1, p. e12922, Jan. 2023, doi: 10.1016/j.heliyon.2023.E12922.
- [4] S. Sikiru, T. T. Dele-Afolabi, M. Yeganeh Ghotbi, and Z. U. Rehman, “Recent advancements in technology projection on electric double layer effect in battery recycling for energy storage,” *Journal of Power Sources*, vol. 596, p. 234056, Mar. 2024, doi: 10.1016/j.jpowsour.2024.234056.
- [5] H. Maghfiroh, O. Wahyunggoro, and A. I. Cahyadi, “Low Pass Filter as Energy Management for Hybrid Energy Storage of Electric Vehicle: A Survey,” *Automotive Experiences*, vol. 6, no. 3, pp. 466–484, 2023, doi: 10.31603/ae.9398.
- [6] A. D. Shieddieque, I. Rahayu, S. Hidayat, and J. A. Laksmono, “Recent Development in LiFePO<sub>4</sub> Surface Modifications with Carbon Coating from Originated Metal-Organic Frameworks (MOFs) to Improve the Conductivity of Cathode for Lithium-Ion Batteries: A Review and Bibliometrics Analysis,” *Automotive Experiences*, vol. 6, no. 3, pp. 438–451, 2023, doi: 10.31603/ae.9524.
- [7] J. E. Y. Mei, C. Feng, J. Ding, L. Cai, and B. Luo, “A review of enhancing micro combustion to improve energy conversion performance in micro power system,” *International Journal of Hydrogen Energy*, vol. 47, no. 53, pp. 22574–22601, Jun. 2022, doi: 10.1016/j.ijhydene.2022.05.042.
- [8] S. Sheykhbaglou, A. Ghahremani, S. Tabejamaat, and M. Sánchez-Sanz, “Comparative study of combustion and thermal performance of a meso-scale combustor under co- and counter-rotating fuel and oxidizer swirling flows for micro power generators,” *Heliyon*, vol. 10, no. 2, p. e24250, Jan. 2024, doi: 10.1016/j.heliyon.2024.e24250.
- [9] X. Yu, N. S. Sandhu, Z. Yang, and M. Zheng, “Suitability of energy sources for automotive application – A review,” *Applied Energy*, vol. 271, p. 115169, Aug. 2020, doi: 10.1016/j.apenergy.2020.115169.
- [10] P. Qian et al., “Experimental study on a high efficient and ultra-lean burn meso-scale thermoelectric system based on porous media combustion,” *Energy Conversion and Management*, vol. 234, p. 113966, Apr. 2021, doi: 10.1016/j.enconman.2021.113966.
- [11] B. Bazooyar and H. Gohari Darabkhani, “Analysis of flame stabilization to a thermophotovoltaic micro-combustor step in turbulent premixed hydrogen flame,” *Fuel*, vol. 257, p. 115989, Dec. 2019, doi: 10.1016/j.fuel.2019.115989.
- [12] J. Wan and A. Fan, “Recent progress in flame stabilization technologies for combustion-based micro energy and power systems,” *Fuel*, vol. 286, p. 119391, Feb. 2021, doi: 10.1016/j.fuel.2020.119391.
- [13] A. Sanata, L. Yuliati, M. N. Sasongko, and I. N. G. Wardana, “Flame behavior inside constant diameter cylindrical meso-scale combustor with different backward facing step size,” *Eastern-European Journal of Enterprise Technologies*, vol. 2, no. 8–104, pp. 44–51, 2020, doi: 10.15587/1729-4061.2020.197988.
- [14] I. Schoegl, V. M. Sauer, and P. Sharma, “Predicting combustion characteristics in externally heated micro-tubes,” *Combustion and Flame*, vol. 204, pp. 33–48, Jun. 2019, doi: 10.1016/j.combustflame.2019.02.029.
- [15] S. N. R. Isfahani, V. M. Sauer, and I. Schoegl, “Effects of dilution and pressure on combustion characteristics within externally heated micro-tubes,” *Proceedings of the Combustion Institute*, vol. 38, no. 4, pp. 6695–6702, Jan. 2021, doi: 10.1016/j.proci.2020.06.090.
- [16] J. Wei et al., “Investigation on hydrogen-fueled combustion characteristics and thermal performance in a micro heat-recirculation combustor inserted with block,” *International Journal of Hydrogen Energy*, vol. 46, no. 73, pp. 36515–36527, Oct. 2021, doi: 10.1016/j.ijhydene.2021.08.145.
- [17] J. Li, H. Xiao, Q. Li, and J. Shi, “Heat recirculation and heat losses in porous micro-combustors: Effects of wall and porous media properties and combustor dimensions,” *Energy*, vol. 220, p. 119772, Apr. 2021, doi: 10.1016/j.energy.2021.119772.

- 10.1016/j.energy.2021.119772.
- [18] L. Gao, T. Cai, A. Tang, and H. Liu, "Effect of hetero-/homogenous combustion on energy conversion performances and flame stability of methane/air-fueled micro-combustors with heat-recirculating structure and platinum-coated," *Fuel*, vol. 349, p. 128610, Oct. 2023, doi: 10.1016/j.fuel.2023.128610.
- [19] M. Bajelani, M. R. Ansari, and E. Nadimi, "A comprehensive study of effective parameters on the thermal performance of porous media micro combustor in thermo photovoltaic systems," *Applied Thermal Engineering*, vol. 231, p. 120846, Aug. 2023, doi: 10.1016/j.applthermaleng.2023.120846.
- [20] H. Wang, Q. Peng, X. Tian, F. Yan, D. Wei, and H. Liu, "Experimental and numerical investigation on H<sub>2</sub>-fueled micro-thermophotovoltaic with CH<sub>4</sub> and C<sub>3</sub>H<sub>8</sub> blending in a tube fully/partially inserted porous media," *Renewable and Sustainable Energy Reviews*, vol. 191, p. 114134, Mar. 2024, doi: 10.1016/j.rser.2023.114134.
- [21] A. Tolouei and A. Gharehghani, "Numerical investigation of premixed methane-ammonia combustion in a mesoscale porous combustor," *Fuel*, vol. 366, p. 131427, Jun. 2024, doi: 10.1016/j.fuel.2024.131427.
- [22] E. Lin, C. T. Wilson, A. Leroy, and B. El Fil, "High energy density entrainment-based catalytic micro-combustor for portable devices," *Energy Conversion and Management*, vol. 285, p. 117014, Jun. 2023, doi: 10.1016/j.enconman.2023.117014.
- [23] A. Mandal, S. Sarkar, A. Chakravarty, and A. Mukhopadhyay, "Flame stabilization and formation of flame street in a H<sub>2</sub>/Air non-premixed micro-combustor with a bluff body," *International Journal of Hydrogen Energy*, vol. 58, pp. 1149–1159, Mar. 2024, doi: 10.1016/j.ijhydene.2024.01.333.
- [24] H. Y. Nanlohy, I. N. G. Wardana, N. Hamidi, L. Yuliati, and T. Ueda, "The effect of Rh<sup>3+</sup> catalyst on the combustion characteristics of crude vegetable oil droplets," *Fuel*, vol. 220, 2018, doi: 10.1016/j.fuel.2018.02.001.
- [25] A. Sanata, I. Sholahuddin, and H. Y. Nanlohy, "Characterization of Biogas as an Alternative Fuel in Micro-Scale Combustion Technology," *International Journal of Integrated Engineering*, vol. 15, no. 4, pp. 64–76, 2023, doi: 10.30880/ijie.2023.15.04.006.
- [26] S. Cai, W. Yang, and J. Wan, "Combustion and thermal performances of methane-air premixed flame in a novel preheated micro combustor with a flame holder," *International Journal of Thermal Sciences*, vol. 197, p. 108813, Mar. 2024, doi: 10.1016/j.ijthermalsci.2023.108813.
- [27] J. Wan and H. Zhao, "Flammability limit of methane-air nonpremixed mixture in a micro preheated combustor with a flame holder," *Chemical Engineering Science*, vol. 227, p. 115914, Dec. 2020, doi: 10.1016/j.ces.2020.115914.
- [28] Q. Peng et al., "Experimental and numerical investigation of a micro-thermophotovoltaic system with different backward-facing steps and wall thicknesses," *Energy*, vol. 173, pp. 540–547, Apr. 2019, doi: 10.1016/j.energy.2019.02.093.
- [29] A. Sanata, I. N. G. Wardana, L. Yuliati, and M. N. Sasongko, "Effect of Backward Facing Step On Combustion Stability in a Constant Contact Area Meso-Scale Combustor," *Eastern-European Journal of Enterprise Technologies*, vol. 1, no. 8 (97), pp. 51–59, 2019, doi: 10.15587/1729-4061.2019.149217.
- [30] Q. Li, J. Li, J. Shi, and Z. Guo, "Effects of heat transfer on flame stability limits in a planar micro-combustor partially filled with porous medium," *Proceedings of the Combustion Institute*, vol. 37, no. 4, pp. 5645–5654, Jan. 2019, doi: 10.1016/j.proci.2018.06.023.
- [31] H. Y. Nanlohy, I. N. G. Wardana, M. Yamaguchi, and T. Ueda, "The role of rhodium sulfate on the bond angles of triglyceride molecules and their effect on the combustion characteristics of crude jatropa oil droplets," *Fuel*, vol. 279, p. 118373, 2020, doi: 10.1016/j.fuel.2020.118373.
- [32] X. Hu, Z. Shen, and Y. Wang, "On the design of a hydrogen micro-rectangular combustor for portable thermoelectric generators," *Chemical Engineering and Processing - Process Intensification*, vol. 195, p. 109611, Jan. 2024, doi: 10.1016/j.cep.2023.109611.
- [33] F. Tohidi, S. Ghazanfari Holagh, and A. Chitsaz, "Thermoelectric Generators: A comprehensive review of characteristics and

- applications," *Applied Thermal Engineering*, vol. 201, p. 117793, Jan. 2022, doi: 10.1016/j.applthermaleng.2021.117793.
- [34] J. Li, J. E. J. Ding, L. Cai, and B. Luo, "Effect analysis on combustion performance enhancement of the hydrogen-fueled micro-cylindrical combustors with twisted tapes for micro-thermophotovoltaic applications," *International Journal of Hydrogen Energy*, vol. 49, pp. 725–743, Jan. 2024, doi: 10.1016/j.ijhydene.2023.09.041.
- [35] P. Abbaspour and A. Alipoor, "Numerical study of wavy-wall effects on premixed H<sub>2</sub>/air flammability limits, propagation modes, and thermal performance of micro combustion chambers," *Applied Energy*, vol. 359, p. 122727, Apr. 2024, doi: 10.1016/j.apenergy.2024.122727.
- [36] C. Zhang *et al.*, "Numerical study on combustion characteristics and heat transfer enhancement of the micro combustor embedded with Y-shaped fin for micro thermo-photovoltaic system," *Applied Thermal Engineering*, vol. 211, p. 118427, Jul. 2022, doi: 10.1016/j.applthermaleng.2022.118427.
- [37] E. K. Quaye, J. Pan, Q. Lu, Y. Zhang, and Y. Wang, "Combustion optimization in consolidated porous media for thermo-photovoltaic system application Using Response Surface Methodology," *International Journal of Thermal Sciences*, vol. 184, p. 107950, Feb. 2023, doi: 10.1016/j.ijthermalsci.2022.107950.
- [38] X. Yang, B. Yu, X. Peng, and H. Zhou, "Investigation of thermal performance and energy conversion in a novel planar micro-combustor with four-corner entrances for thermo-photovoltaic power generators," *Journal of Power Sources*, vol. 515, p. 230625, Dec. 2021, doi: 10.1016/j.jpowsour.2021.230625.
- [39] G. Yang and A. Fan, "Experimental study on combustion characteristics of n-C<sub>4</sub>H<sub>10</sub>/air mixtures in a meso-scale tube partially filled with wire mesh," *Fuel*, vol. 319, p. 123783, Jul. 2022, doi: 10.1016/j.fuel.2022.123783.
- [40] C. Jiang, J. Pan, H. Yu, Y. Zhang, Q. Lu, and E. K. Quaye, "Effects of mixing ozone on combustion characteristics of premixed methane/oxygen in meso-scale channels," *Fuel*, vol. 312, p. 122792, Mar. 2022, doi: 10.1016/j.fuel.2021.122792.
- [41] L. Cai, J. E. J. Li, J. Ding, and B. Luo, "A comprehensive review on combustion stabilization technologies of micro/meso-scale combustors for micro thermophotovoltaic systems: Thermal, emission, and energy conversion," *Fuel*, vol. 335, p. 126660, Mar. 2023, doi: 10.1016/j.fuel.2022.126660.
- [42] J. Tong, T. Cai, and D. Zhao, "Optimizing thermal performances and NO<sub>x</sub> emission in a premixed ammonia-hydrogen blended meso-scale combustor for thermophotovoltaic applications," *International Journal of Hydrogen Energy*, vol. 48, no. 77, pp. 30191–30204, Sep. 2023, doi: 10.1016/j.ijhydene.2023.04.163.
- [43] B. Luo, J. Chen, J. E. G. Liao, F. Zhang, and J. Ding, "Effects of different channels on performance enhancement of a nozzle hydrogen-fueled micro combustor for micro-thermophotovoltaic applications," *International Journal of Hydrogen Energy*, vol. 48, no. 54, pp. 20743–20761, Jun. 2023, doi: 10.1016/j.ijhydene.2023.03.025.
- [44] X. Zhu, Z. Zhao, Z. Zuo, B. Jia, W. Wang, and P. Xu, "Experimental studies on the role of thermoelectric module structure in developing a powerful miniature power generator with a meso-scale opposed flow porous combustor," *Applied Thermal Engineering*, vol. 230, p. 120586, Jul. 2023, doi: 10.1016/j.applthermaleng.2023.120586.
- [45] C. Zhang, Y. Yan, K. Shen, Z. Xue, J. You, and Z. He, "Comparative analysis of combustion stability and flow performance in micro combustor based on the synergistic action of slotted blunt body and front-baffle," *Applied Thermal Engineering*, vol. 237, p. 121802, Jan. 2024, doi: 10.1016/j.applthermaleng.2023.121802.